

# A Numerical Study on Heat Transfer in Laminar Pulsed Slot Jets Impinging on a Surface

D. Kim

**Abstract**—Numerical simulations are performed for laminar continuous and pulsed jets impinging on a surface in order to investigate the effects of pulsing frequency on the heat transfer characteristics. The time-averaged Nusselt number of pulsed jets is larger in the impinging jet region as compared to the continuous jet, while it is smaller in the outer wall jet region. At the stagnation point, the mean and RMS Nusselt numbers become larger and smaller, respectively, as the pulsing frequency increases. Unsteady behaviors of vortical fluid motions and temperature field are also investigated to understand the underlying mechanisms of heat transfer enhancement.

**Keywords**—Pulsed slot jet, impingement, pulsing frequency, heat transfer enhancement.

## I. INTRODUCTION

IMPINGING jets [1, 2] have been widely used in many industrial applications because they provide an effective way to enhance heat and mass transfer. For example, applications include rapid cooling/heating processes, drying of papers, films, and foods, and tempering of glass and metal. The advantage of jet impingement is its ease to adjust the location of interest and to remove a large amount of heat and mass from the impinging surface due to the thin thermal and concentration boundary layers around the stagnation region.

In recent years, researchers have paid attention to the potential of heat transfer enhancement using flow pulsation [3-5]. So far, there have been many attempts to obtain heat transfer enhancement and optimal conditions of pulsed impinging jets. However, previous experimental and numerical results show conflicting results. Some researchers reported a marginal or significant heat transfer enhancement by means of jet pulsation, but others showed no enhancement or even deterioration [3]. Furthermore, flow instability, chaotic mixing, higher turbulence level, etc. are believed to be possible reasons for enhancement [5], but it is still unclear. In addition, previous studies are mostly concerned with high Reynolds number jets, and thus studies on laminar pulsed jets are needed.

Therefore, in this study, the fluid flow and thermal fields are numerically simulated for laminar pulsed jets impinging on a surface. We aim at investigating the effects of pulsating frequency on the heat transfer along the impinging surface and the underlying reasons for enhancement or deterioration.

D. Kim is with Department of Mechanical Engineering, Kumoh National Institute of Technology, Gumi, Gyeongbuk 730-701, Korea (phone: 82-54-478-7301; fax: 82-54-478-7319; e-mail: kdj@kumoh.ac.kr).

## II. NUMERICAL MODEL

A two-dimensional impinging jet configuration is modeled as shown in Fig. 1. The jet is vertically injected down from the slot nozzle and then it impinges on the bottom wall. In this study, we consider a semi-confined case with a confinement wall parallel to the impingement wall. It is assumed that the flow is 2-D, laminar, incompressible, and fluid properties are constant independent of temperature. Therefore, the governing equations for fluid flow and thermal fields of pulsed jets are written as

$$\frac{\partial u_i}{\partial x_i} = 0, \quad (1)$$

$$\rho \left[ \frac{\partial u_i}{\partial t} + \frac{\partial (u_i u_j)}{\partial x_j} \right] = - \frac{\partial p}{\partial x_i} + \mu \frac{\partial^2 u_i}{\partial x_j \partial x_j}, \quad (2)$$

$$\rho C_p \left[ \frac{\partial T}{\partial t} + \frac{\partial (u_i T)}{\partial x_i} \right] = k \frac{\partial^2 T}{\partial x_j \partial x_j}. \quad (3)$$

Here,  $u_i$ ,  $p$ , and  $T$  are velocity vector, pressure, and temperature, respectively. The gravity and buoyancy forces are not considered in this study. The governing equations are solved with the finite volume CFD code, FLUENT. The third-order QUICK scheme is used for convection terms in the momentum and energy equations, and the SIMPLE algorithm is adopted for the pressure-velocity coupling.

Fig. 1(a) shows the coordinate system, computational domain and boundary conditions. The Cartesian coordinate system is used and its origin is located at the center of impingement wall. The computational domain is  $-15w \leq x \leq 15w$ ,  $0 \leq y \leq H$ , where  $w$  is the jet width and  $H(=5w)$  is the distance between the jet nozzle and impingement wall. A spatially uniform velocity with time variation of square waveform like Fig. 1(b) is specified at the jet inlet, and the pressure outlet boundary condition is used at the outlet. The temperature of jet flow is assumed to be lower than that of isothermal impingement wall, and the confinement wall is considered to be adiabatic. A non-uniform mesh is used with dense resolution near the solid surface and the pulsed jet. The total number of grid points used is  $271(x) \times 101(y)$  which is determined from a grid independence test.

Simulations are performed for  $Re=50$  and  $Pr=0.7$ , where  $Re$  is based on the jet width and time-averaged jet velocity  $U_{avg}$ . The dimensionless pulsing frequency  $St(=fw/U_{avg})$  is varied from 0.05 to 0.5. The duty cycle, denoting the time fraction where the jet is injected from the nozzle, is fixed to be 50%.

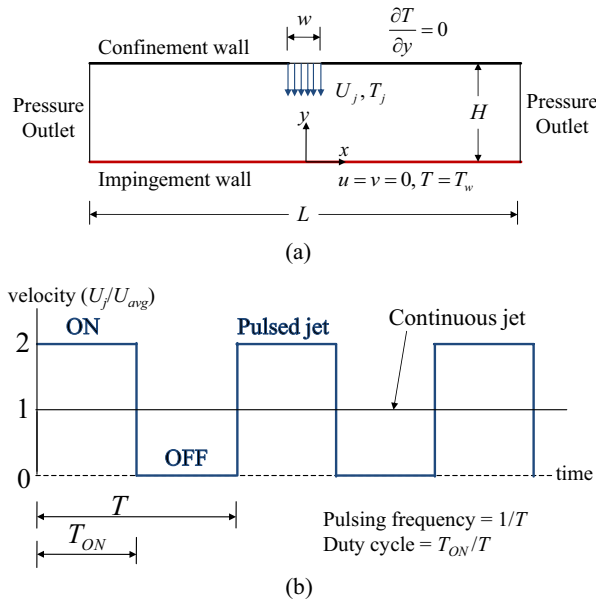


Fig. 1 Numerical model: (a) coordinate system, computational domain, and boundary conditions; (b) jet velocity profile of continuous and pulsed jets

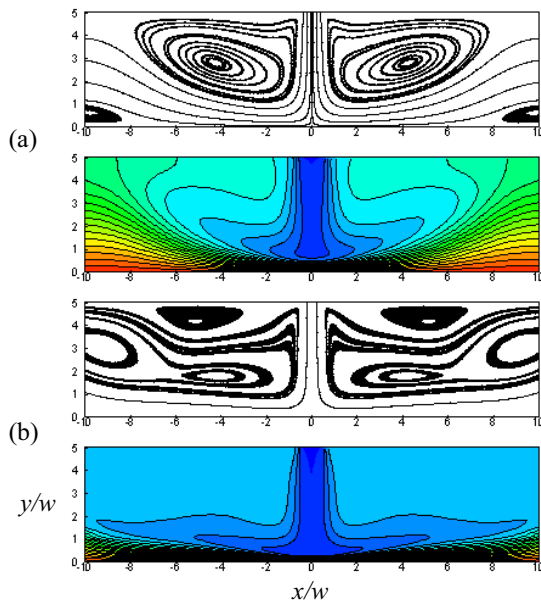


Fig. 2 Streamlines (upper) and temperature contours (lower) for continuous jets: (a)  $Re=50$ ; (b)  $Re=150$

### III. RESULTS

Continuous jets are first simulated in order to verify the present numerical method before simulating pulsed jets. Fig. 2 shows the streamlines and temperature contours at two different Reynolds numbers of 50 and 150. At  $Re=50$ , in addition to main recirculating vortices near the jet inlet, secondary vortices are found at  $|x| \sim 10w$  on the lower wall. However, at  $Re=150$ , main

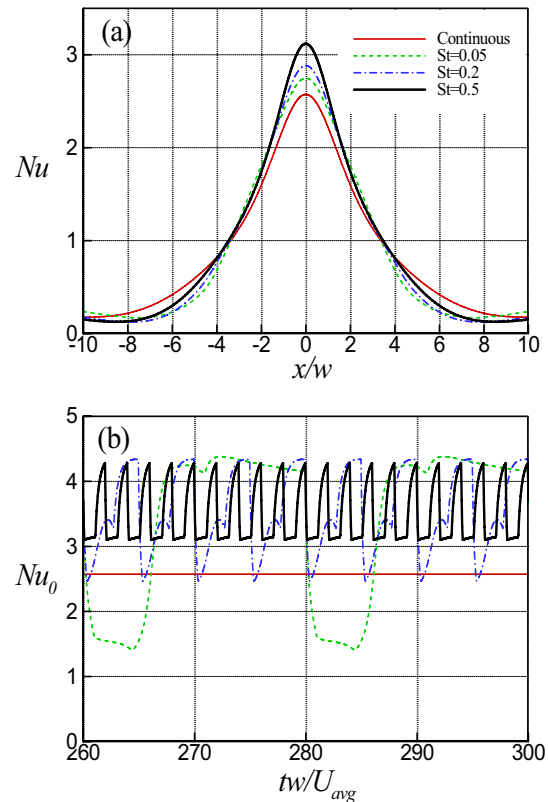


Fig. 3 Variations of Nusselt number depending on the pulsing frequency: (a) time-averaged value along the impingement wall; (b) time history of instantaneous value at the stagnation point

recirculating vortices are separated into two parts and secondary vortices occur on the upper wall. This difference in fluid vortical motions leads to different characteristics of the temperature distribution and convective heat transfer on the impingement wall. For example, the thermal boundary layer at  $Re=50$  is much larger than that at  $Re=150$  far away from the stagnation point. The Nusselt number at the stagnation point obtained in this study is 2.57 and 5.53, respectively, at  $Re=50$  and 150. The present results are in good agreement with the previous results [2] qualitatively and quantitatively.

Now, pulsed jets are simulated for  $Re=50$  and compared with the results of continuous jet. Fig. 3(a) shows the time-averaged Nusselt number along the impingement wall. For both of continuous and pulsed jets, the mean Nusselt number is largest at the stagnation point and it decreases with the distance from that point. It is also clear that the effect of jet pulsation depends on the  $x$  location. Near the stagnation point ( $|x| < 3w$ ), the mean Nusselt number of pulsed jets is larger than that of continuous jet, whereas it is smaller at outer wall jet region.

Unsteady behaviors of stagnation Nusselt number are examined by the time history shown in Fig. 3(b). One can clearly see the variations corresponding to the pulsing frequency for all the pulsed jets considered. From this figure, it can be confirmed that the mean Nusselt number increases with

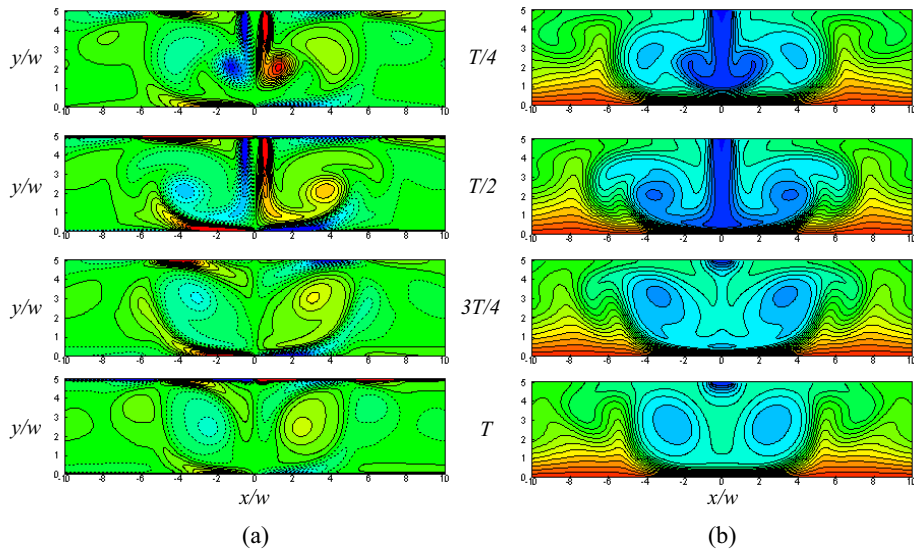


Fig. 4 Time sequence of contours during a pulsing period  $T$  for  $St=0.05$ : (a) spanwise vorticity; (b) temperature

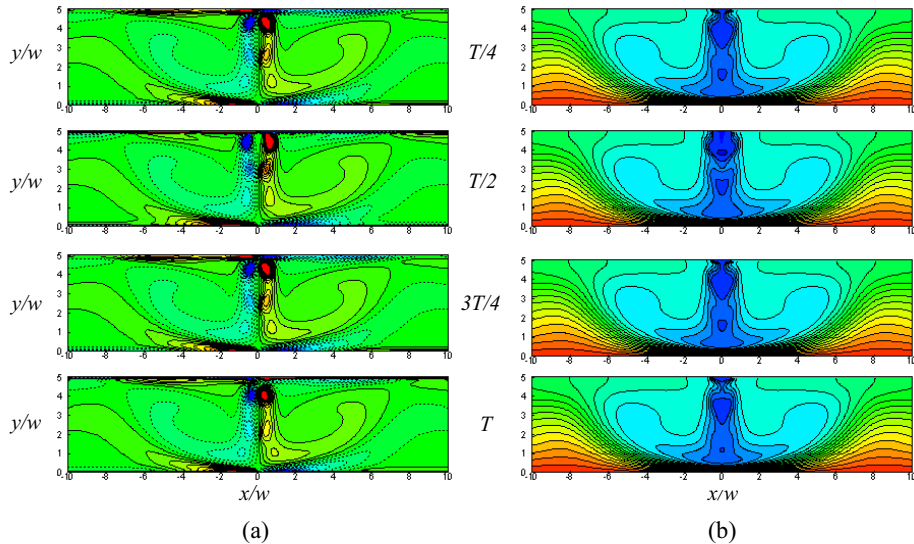


Fig. 5 Time sequence of contours during a pulsing period  $T$  for  $St=0.5$ : (a) spanwise vorticity; (b) temperature

the pulsing frequency. This observation is very similar to that found in turbulent pulsed impinging jets [5]. Meanwhile, the RMS(Root-Mean-Square) Nusselt number becomes smaller as the pulsing frequency gets larger.

In order to figure out the underlying reasons for the effects of pulsing frequency on the mean and RMS Nusselt numbers, unsteady behaviors of spanwise vorticity and temperature contours are closely investigated. Figs. 4 and 5 show time sequence of those contours during a pulsing period for  $St=0.05$  and  $0.5$ , respectively. According to Sau & Mahesh [6], the stroke ratio (ratio of stroke length to nozzle diameter) is one of the important parameters of pulsed jets in crossflow and it becomes the inverse of the pulsing Strouhal number in the case of 100% modulation. The present flow is different from that of

[6], but the stroke length (or ratio) of pulsed jets is believed to be still important in understanding this type of flow. At  $St=0.05$ , the stroke length is 20 times nozzle width, i.e., much larger than the distance between nozzle and impingement wall. Therefore, a large vortex pair induced by the pulsation hits on the wall before next one is generated, and it recirculates near the center region interacting with the next one. This large and strong recirculation leads to significant temporal variations in the temperature field and a relatively smaller mean Nusselt number at the stagnation point. On the other hand, at  $St=0.5$ , the stroke length is twice nozzle width, i.e., smaller than the nozzle-to-wall distance. Thus, this high-frequency pulsation generates a street of smaller vortex pairs along the jet centerline before the interaction with the impingement wall takes place. The

recirculation of jet vortices after the impingement is relatively weak and temporal variations of temperature field are less significant compared with the low frequency case of  $St=0.05$ .

#### IV. CONCLUSIONS

Fluid flow and thermal fields of laminar continuous and pulsed jets impinging on a surface are numerically simulated. In the case of pulsed jets, the pulsing frequency is varied to examine its effect on the heat transfer along the impingement wall. The present numerical method is verified by comparing the present results for continuous jet with previous ones. Near the stagnation point, heat transfer enhancement is clearly obtained with pulsed jets. That is, the time-averaged Nusselt number increases with increasing pulsing frequency for all the cases considered. However, the RMS Nusselt number at the stagnation point decreases with the pulsing frequency. These observations are closely related to unsteady evolution of vortical fluid motions that is explained with the consideration of stroke length of pulsed jets relative to the nozzle-to-wall distance.

#### ACKNOWLEDGMENT

This research was supported by Basic Research Program through the National Research Foundation of Korea (NRF) funded by the Ministry of Education, Science and Technology (No. 2010-0010936).

#### REFERENCES

- [1] V. A. Chiriac, and A. Ortega, "A numerical study of the unsteady flow and heat transfer in a transitional confined slot jet impinging on an isothermal surface," *Int. J. Heat Mass Tran.*, vol. 45, 2002, pp. 1237-1248.
- [2] H. G. Lee, H. S. Yoon, and M. Y. Ha, "A numerical investigation on the fluid flow and heat transfer in the confined impinging slot jet in the low Reynolds number region for different channel heights," *Int. J. Heat Mass Tran.*, vol. 51, 2008, pp. 4055-4068.
- [3] H. J. Poh, K. Kumar, and A. S. Mujumdar, "Heat transfer from a pulsed laminar impinging jet," *Int. Commun. Heat Mass*, vol. 32, 2005, pp. 1317-1324.
- [4] R. C. Behera, P. Dutta, and K. Srinivasan, "Numerical study of interrupted impinging jets for cooling of electronics," *IEEE T. Compon. Pack. T.*, vol. 30, 2007, pp. 275-284.
- [5] P. Xu, B. Yu, S. Qiu, H. J. Poh, and A. S. Mujumdar, "Turbulent impinging jet heat transfer enhancement due to intermittent pulsation," *Int. J. Therm. Sci.*, vol. 49, 2010, pp. 1247-1252.
- [6] R. Sau, and K. Mahesh, "Optimization of pulsed jets in crossflow," *J. Fluid Mech.*, vol. 653, 2010, pp. 365-390.